

An exact general remeshing scheme applied to physically conservative voxelization

Devon Powell^a, Tom Abel^a

^a*Kavli Institute for Particle Astrophysics and Cosmology, Stanford University, SLAC National Accelerator
Laboratory, Menlo Park, CA 94025, USA*

Abstract

We present an exact general remeshing scheme to compute analytic integrals of polynomial functions over the intersections between convex polyhedral cells of old and new meshes. In physics applications this allows one to ensure global mass, momentum, and energy conservation while applying higher-order polynomial interpolation. We elaborate on applications of our algorithm arising in the analysis of cosmological N-body data, computer graphics, and continuum mechanics problems.

We focus on the particular case of remeshing tetrahedral cells onto a Cartesian grid such that the volume integral of the polynomial density function given on the input mesh is guaranteed to equal the corresponding integral over the output mesh. We refer to this as “physically conservative voxelization”.

At the core of our method is an algorithm for intersecting two convex polyhedra by successively clipping one against the faces of the other. This algorithm is an implementation of the ideas presented abstractly by Sugihara (1994), who suggests using the planar graph representations of convex polyhedra to ensure topological consistency of the output. This makes our implementation robust to geometric degeneracy in the input. We employ a simplicial decomposition to calculate moment integrals up to quadratic order over the resulting intersection domain.

We also address practical issues arising in a software implementation, including numerical stability in geometric calculations, management of cancellation errors, and extension to two dimensions. In a comparison to recent work, we show substantial performance gains. We provide a C implementation intended to be a fast, accurate, and robust tool for geometric calculations on polyhedral mesh elements.

Keywords: remesh, remap, rasterization, voxelization, conservative, dark matter, plasma, Vlasov, Poisson, hydrodynamics

1. Introduction

Several areas of computational physics require one to remesh (also “remap” or “resample”) physical quantities between meshes made of convex polyhedra in a physically conservative manner. By “physically conservative,” we mean that mesh cells from the old and new meshes are overlain, the volumes of intersection between old and new cells constructed, and the quantity of interest transferred from the old to the new mesh cells such that the total integral over the output and input are equal.

One instance of this is in numerical hydrodynamics, where a highly distorted mesh must be relaxed and remeshed in order to avoid loss of accuracy. In this context, the subject of this paper is known as a “direct remap.” This is of interest in some flavors of Arbitrary Lagrangian-Eulerian (ALE) hydrodynamics (see e.g. Donea et al. 2004) and, more recently, in the “re-ALE” scheme pioneered by Loubère et al. (2010). The precise problem of intersecting arbitrary polyhedra for direct remapping of hydrodynamical quantities is attacked by Grandy (1999), who gives a description of a first-order scheme for polyhedral grids, as well as a thorough review of the topic. Dukowicz and Kodis (1987) and Dukowicz et al. (1991) present algorithms for the same problem, including higher-order interpolation during the remap step.

Interface reconstruction for multiphase flows (specifically, piecewise-linear interface reconstruction, or PLIC) relies on calculating the volume of a mesh cell that has been truncated against the interface plane. This is akin to the intersection of two polyhedra, though in this case the problem is restricted to intersecting a polyhedron with another plane. Hirt and Nichols (1981) describe the so-called “volume-of-fluid” (VOF) methods, which enforce volume conservation of material in a grid cell during this clipping operation. Renardy et al. (2001) provide a good overview of the basic concepts involved. López and Hernández (2008) give a Fortran toolkit of the necessary operations for VOF, against which we give a direct comparison in the results section.

A physically conservative remesh is also useful for visualization purposes. Specifically, we refer to “voxelization” (also “scan-line conversion” or “rasterization”), a geometric operation in which polyhedra are mapped onto a 3D Cartesian lattice of cubical grid cells (“voxels”). The current state-of-the-art in voxelization as a computer graphics application is given by Duff (1989), who generates anti-aliased images by computing exact convolution integrals for separable polynomial filters. More recently, Auzinger et al. (2012) and Auzinger and Wimmer (2013) compute exact convolution integrals for non-separable (spherically-symmetric) polynomial filters. Catmull (1978) describes area-sampling in 2D, which is equivalent to convolving the continuous image with the pixel shape. Again, the problem of intersecting convex polyhedra arises, as voxelization on a conceptual level is simply the computation of integrals over the intersection volumes between cubical grid cells and input polyhedra.

The particular application for which we developed the method presented here is the exact mass-conservative voxelization of tetrahedra for the simulation and analysis of cosmological N -body systems using the method of Abel et al. (2012). This approach to the N -body problem treats dark matter particles as tracers, and interprets the mass as being interpolated between the tracers in tetrahedral mass elements. This approach has the advantage of giving a well-defined density field everywhere in space, eliminating the need to consider particle discreteness effects. It has since been explored in more detail by Angulo et al. (2014), who create smooth maps of the gravitational lensing potential around dark matter halos, Hahn et al. (2013), who show that this method eliminates artificial clumping in N -body simulations, and Hahn et al. (2014), who look at statistics of cosmic velocity fields. Kaehler et al. (2012) use voxelization in a visualization context to produce stunning and informative renderings of cosmic structures.

We refer in this paper to the specific case of “physically conservative voxelization” of tetrahedra, in which a scalar density defined across the input tetrahedron is integrated over each domain formed by the intersection of the tetrahedron with each grid cell that intersects

the tetrahedron (see Figures 1 and 2 for illustrations). Hence, the sum over each voxel in the output should exactly equal the total integral over the input.

Thus, this paper describes a specific application of a physically conservative remesh, while remaining cognizant of the fact that the concepts presented here form a general conservative remesh scheme applicable to any of the aforementioned problems. Our goal is to present a unified approach for intersecting two convex polyhedra in a geometrically robust way, and for accurately computing the integral of a polynomial function over the resulting intersection domain.

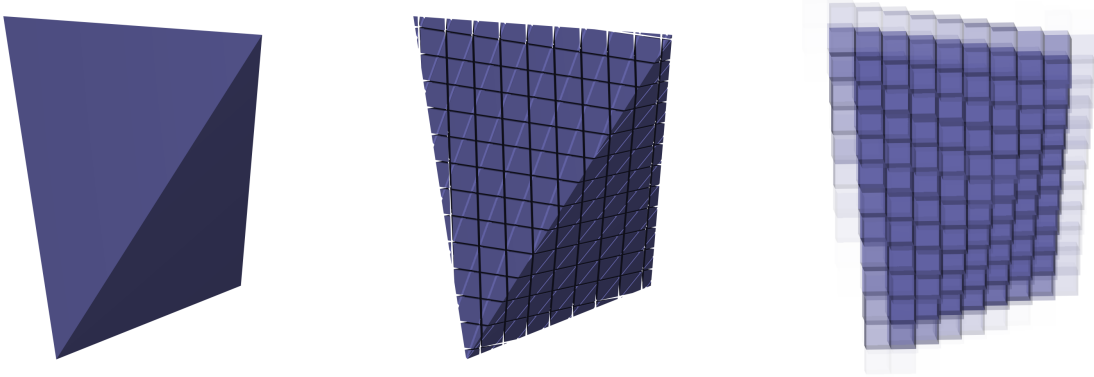


Figure 1: An illustration of physically conservative voxelization. Left: An input tetrahedron. Middle: The input tetrahedron, split between underlying cubical grid cells (voxels) to form a set of non-overlapping integration domains, each of which is the intersection of a cube and the tetrahedron. Right: the voxelized tetrahedron. The total volume integral is conserved to high precision between the left and right figures.

As we discuss in Section 3, there are two basic operations that form the core of our algorithm: a clipping operation, in which a cube is repeatedly truncated against the faces of a tetrahedron (this is equivalent to intersecting two convex polyhedra), and a reduction operation, in which we integrate a polynomial density over the the convex polyhedron resulting from the clipping operation.

The integration of polynomial fields over arbitrary polyhedral domains has been well-studied in the literature. One approach is to reduce the dimensionality of a volume integral using the divergence theorem. Dukowicz and Kodis (1987), Liggett (1988), Mirtich (1996), and Margolin and Shashkov (2003) all use the divergence theorem to reduce such volume integrals to line integrals. In particular, the two-dimensional case in Cartesian coordinates is well known (Stone 1986), including formulae for moments over the polygons (Bockman 1989). A second approach to this problem is to decompose the domain into simplices (tetrahedra in 3D, triangles in 2D) and carry out the integration over each simplex separately using existing formulae derived using barycentric coordinates (see Section 3.3). This method is well-established in implementations of the finite element method (FEM), where mesh elements are often simplices. Most recently, De Loera et al. (2011) present software for the exact integration of polynomials over convex polyhedral domains using simplicial decomposition. Liu and Vinokur (1998) present a similar algorithm.

The clipping operation is more subtle. The classic method for clipping a polyhedron

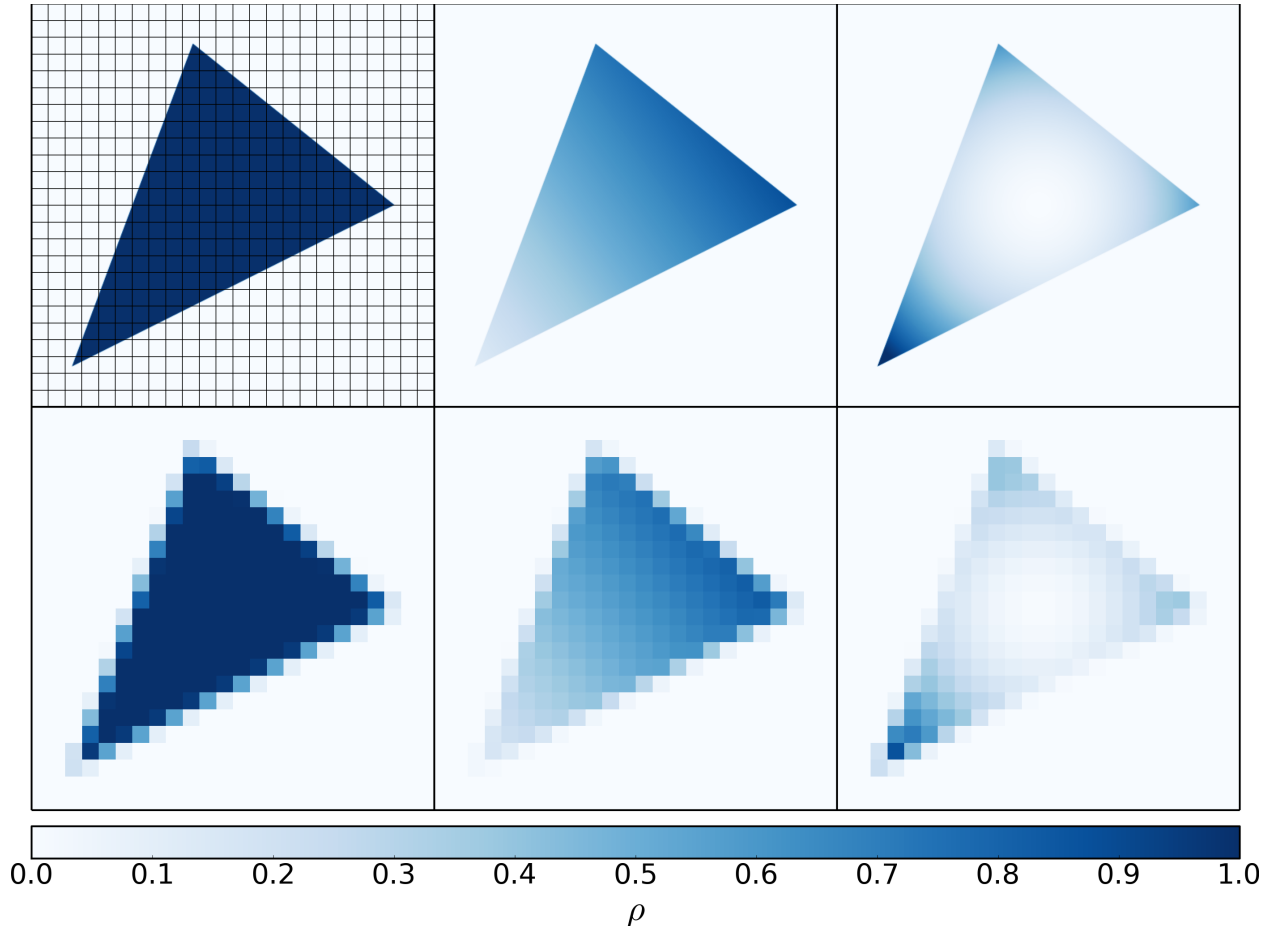


Figure 2: Another illustration of physically conservative voxelization. Here we show slices through a voxelized triangular prism with constant (left), linear (middle) and quadratic (right) density fields defined over the domain. Top row: The input, with continuous polynomial density. The top-left panel also shows the grid to which we are voxelizing. Bottom row: The voxelized output. Mass is conserved to high precision between the top and bottom rows.

against a plane is Sutherland-Hodgman clipping (Sutherland and Hodgman 1974), which simply tests vertices against the clip plane and excludes those vertices lying on the “wrong” side. This method requires some sort of lookup table for reconstructing the boundary connectivity of the resulting polyhedron, as implemented by Stephenson and Christiansen (1975). However, this method is not geometrically robust, meaning that it can admit geometrical inconsistencies if vertices lie on the clip plane to within roundoff error. In this case, vertices may be duplicated or omitted, giving an invalid representation for the output polyhedron. This is catastrophic for, say, the integration process, which requires complete and self-consistent geometrical information.

Because ours is a computational physics application, geometrical robustness to the input data is a necessity; we require accurate and conservative output for *all* possible input cases. Previous work in computational physics (e.g. Dukowicz et al. 1991, Grandy 1999) has dealt with this issue by using auxiliary algorithms for detecting and artificially removing

such geometrical ambiguities, or by dealing with them on a case-by-case basis. We instead propose to handle geometric degeneracies in a cleaner way, by implementing an algorithm that is naturally immune to them, and hence manifestly robust.

The question of how to design a geometrically robust method for intersecting polyhedra (intersecting two convex polyhedra is equivalent to repeatedly clipping one against the faces of the other) is addressed in detail by Stewart (1994), who gives a thorough review of the literature. The author divides ways of achieving geometric robustness into three main classes. The first is exact arithmetic, meaning that the input polyhedron is represented exactly (e.g. integer or rational coordinates), removing the possibility of geometric ambiguity from subsequent tests. Either some form of high-precision arithmetic is used (e.g. Sugihara and Iri 1990), or the vertices/edges of an input polyhedron are perturbed in such a way that a finite-precision algorithm can never encounter a geometrically ambiguous decision (e.g. Milenkovic 1988). The second is the representation and model approach developed by Hoffmann et al. (1988), which makes geometric decisions guaranteeing that the mapping from input to output representations always corresponds to valid input and output models. The final class are the topological consistency methods. They work by guaranteeing that the output is always valid in a topological sense. Such methods are not in general provably robust, but empirical tests have shown that they indeed are. Sugihara and Iri (1989) achieve this by eliminating redundant numerical tests. Other examples include Karasick (1989), who employs rules on how geometric intersections are allowed to occur, and Bruderlin (1991), who checks nearby features that may be merged for whether they result in a valid polyhedron.

Our choice of which of these aforementioned algorithms to use for our application is informed by the fact that we want to perform both the clipping and reduction operations on the same polyhedral representation, so as to avoid the extra computation needed in changing representations.

We choose to represent convex polyhedra using their planar graphs and perform the clipping operation in a way that preserves the topological validity of the output graph, as suggested by Sugihara (1994). This is a member of the topological consistency methods, and it ensures that our method is robust by making geometric decisions combinatorially, using numerical comparisons only as a guide. This representation for convex polyhedra lends itself naturally to a simplicial decomposition approach for the integration step, which can be accomplished easily by traversing the graph.

The layout of this paper is as follows. In Section 2, we discuss the original application for this work (the analysis and simulation of dark matter in cosmology), as well as elaborating on other potential applications in computer graphics and hydrodynamics. Section 3 presents in detail the main concepts in the voxelization algorithm, while Section 4 discusses some subtleties arising in a practical implementation. Finally, we present results concerning accuracy, robustness, and performance of our C implementation, comparing to previous work, in Section 5.

2. Motivation

2.1. Cosmological N -body data

The application for which we developed the method presented here is the physically conservative voxelization of tetrahedra for the simulation and analysis of cosmological N -

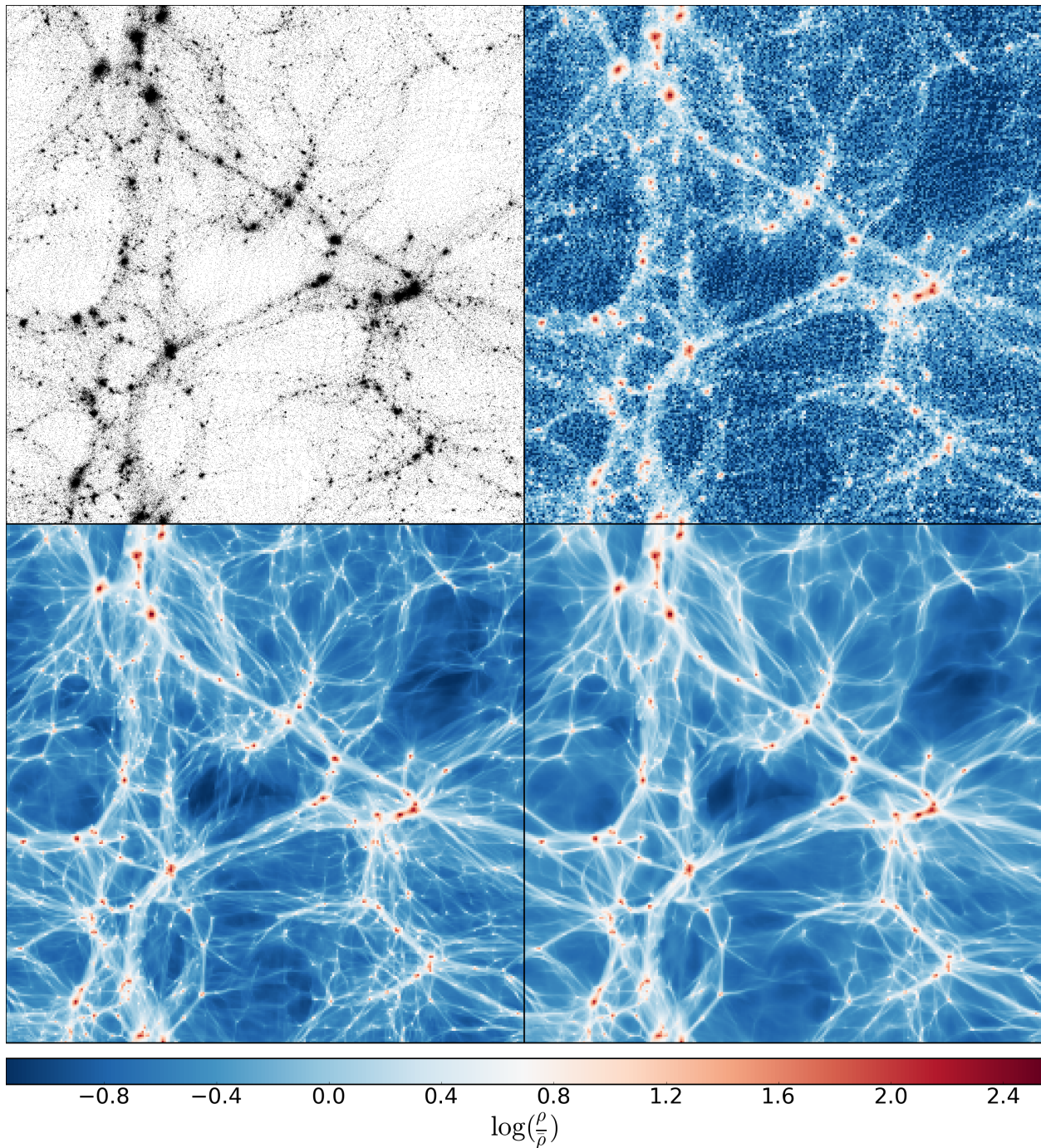


Figure 3: Visual comparison of methods for depositing dark matter mass onto a regular grid. Top left: Scatter plot of particle locations. Top right: Cloud-in-cell (CIC) deposit. Bottom left: Conservative voxelization, with piecewise-constant density. Bottom right: Conservative voxelization, with piecewise-linear density. The bottom two panels use the method of Abel et al. (2012) to properly capture the phase-space structure of the dark matter, using the physically conservative voxelization scheme presented here to conserve mass to machine precision. This is the motivation for the present work.

body systems using the approach of Abel et al. (2012). (See Figure 3.)

Dark matter, like any continuous system in physics, can be represented by a probability distribution function (PDF) in phase space. The computational solution of this system requires the discretization of this continuous PDF, something traditionally done using Dirac- δ -like particles. As such, the results of commonly used N-body codes such as Gadget2 (Springel 2005), HACC (Habib et al. 2012), 2HOT (Warren 2013), Enzo (Bryan et al. 2014), Ramses (Teyssier 2002), NyX (Almgren et al. 2013), and ART (Kravtsov et al. 1997) are given in a particle description. While these codes differ in the ways they compute gravitational forces, decompose the domain, apply force-softening to particles, etc., they are all fundamentally N-body codes that interpret dark matter mass as being concentrated at point locations.

This can be problematic when it comes to the analysis of such N-body data. In many applications (e.g. solution of the Poisson equation, identification of cosmic voids, visualization), we desire the density field to be represented continuously, so that there is no ambiguity in the local density of a particle distribution. Simply binning particles into their nearest grid cell (known as cloud-in-cell, or CIC; see e.g. Hockney and Eastwood 1988) is a ubiquitous technique for doing so, and is traditionally used in the force computation step for particle mesh (PM) codes. Voronoi tessellation around particles has also seen some success (e.g., Neyrinck 2008). However, both of these methods are subject to Poisson counting uncertainty due to their particle nature.

Abel et al. (2012) study N-body (dark matter) simulation data by representing the cold phase-space distribution of dark matter as a three-dimensional “sheet” tessellated into simplices. When modeling a cold fluid in phase space, one only needs to represent a three-dimensional manifold moving in the six-dimensional phase space. The tetrahedral tessellation is thus a piecewise-linear approximation to this smooth Lagrangian three-manifold embedded in \mathbb{R}^6 . Rather than carrying mass themselves, the particle positions serve merely as tracers of the underlying phase-space distribution; the mass itself is interpolated between tracer particles with neighboring Lagrangian coordinates. Such an approach unambiguously gives the density and velocity of the distribution everywhere in configuration space, as opposed to traditional particle-based schemes, which are subject to sampling noise. When the tracer particles move on characteristics and the mass inside the volumes they span can be assumed invariant, the full microphysical phase-space structure is captured by such a three-dimensional sheet.

This scheme has the advantage of giving a well-defined density field everywhere in space, eliminating the need to consider particle discreteness effects. The method has since been explored in more detail by Angulo et al. (2014), who create smooth maps of the gravitational lensing potential around dark matter halos, Hahn et al. (2013), who show that this method eliminates artificial clumping in N-body simulations, and Hahn et al. (2014), who look at statistics of cosmic velocity fields. Kaehler et al. (2012) employ this method in a scientific visualization context, exploring its advantages over a variety of other techniques and discussing some key ways to frame the problem so that primitives of typical computer graphics hardware can be exploited optimally.

This description of dark matter as a collection of mass-carrying tetrahedra is very useful. However, this density field is still represented in Lagrangian space; we require a way to project tetrahedral mass elements onto a Cartesian grid in 3D configuration space.

Angulo et al. (2014) recursively split tetrahedra until each one is smaller than a grid

cell, then deposits the mass to the nearest cell. This conserves mass, but is relatively slow compared to the method described here, and introduces some small-scale noise. Hahn et al. (2013) use a CIC deposit, the mass-conserving particle-based method mentioned above, to generate the density field used in solving the Poisson equation. This method works well for simulating gravitational forces between particles, but is unsuitable for visualization or for more advanced simulation methods such as Hahn and Angulo (2015). Hahn et al. (2014) use a multisampling approach, in which the mass distribution is sampled several times within each grid cell, and the results averaged. This method works very well for visualization and some analysis purposes. However, for certain other applications, including solving for gravitational forces using the Poisson equations, we need the total mass to be conserved.

So, we desire the total mass contained in a grid cell to exactly equal the integral of the input density field over the cell, while avoiding aliasing noise, and to do it quickly and accurately. The problem reduces to finding the integral of a polynomial density field over each domain resulting from the intersection of the input tetrahedron with the cubical grid cells. In other words, we require a physically conservative voxelization scheme for depositing tetrahedral mass elements to a grid.

2.2. Computer graphics and visualization

As discussed in the introduction, another area for which this work may be useful is that of voxelization for computer graphics. This is in the context of computing exact convolution integrals of polynomial filters over cubical cells. In one way or another, Catmull (1978), Duff (1989), Auzinger et al. (2012), and Auzinger and Wimmer (2013) compute such convolution integrals to achieve perfect anti-aliasing in the output images. Our method extends the area-sampling approach of Catmull (1978) to “volume-sampling” in 3D.

Hasselgren et al. (2005), Zhang et al. (2007), and Pantaleoni (2011) describe GPU implementations of “conservative” voxelization. In their context, “conservative” means that each voxel that intersects a polyhedron is correctly identified; however, there is no guarantee that the total volume integral is conserved. Our method could be efficiently combined with these hardware-accelerated collision-finding algorithms to exactly enforce local conservation of physical quantities. This is exciting for scientific visualization applications such as that of Kaehler et al. (2012).

2.3. Hydrodynamics

Generally speaking, numerical hydrodynamics schemes are derived from conservation laws (continuity equations) for mass, momentum, and energy in their integral forms (see Jameson et al. 1981, for example). Hughes (1981) and Donea et al. (2004) describe Arbitrary Lagrangian-Eulerian (ALE) schemes on a moving mesh. A major component in ALE schemes is the remesh, which moves the mesh to some desired updated configuration and reapportions conserved quantities from the old mesh to the new one. This is most often done advectively (the remesh step is absorbed into the hydrodynamics solve), though in some instances a direct (geometric) remap is performed.

Here we must also note that ALE schemes typically use grids whose topology is fixed. In the case of non-simplicial (i.e. hexahedral) grids, this leads to cell faces whose points are not coplanar. In some instances, cells are defined using curvilinear surfaces, giving a higher-order scheme (e.g. Anderson et al. 2015). Others (e.g. Garimella et al. 2007) decompose

faces into triangles to give a consistent, polyhedral description of a mesh cell regardless of topology. One exception is the work of Springel (2010), who solves the hydrodynamic equations on a moving Voronoi mesh, which naturally gives polyhedral cells. Another is the “re-ALE” scheme pioneered by Loubère et al. (2010), in which the mesh topology is not fixed, but is “reconnected” at every timestep to ensure that the mesh remains polyhedral. The applicability of our method is limited to such polyhedral cells.

As we show in Section 3.2, a core component of the method presented here is the clipping operation, in which we construct a convex polyhedron by intersecting a cube with the four face planes comprising a tetrahedron. Although we developed this method and optimized our particular implementation for voxelizing tetrahedra to a grid of uniform cubes, the clipping operation is general and can be applied to any convex polyhedron with an arbitrary number of faces. Hence, it may form the basis for such a direct remap scheme in a hydrodynamics context. We give a demonstration of such a direct first-order remesh in 2D in Section 4.4.

The problem of intersecting arbitrary polyhedra for direct remapping in hydrodynamics has been previously addressed by Grandy (1999), Dukowicz and Kodis (1987), and Dukowicz et al. (1991). The improvement that our method offers over previous work in this area is geometrical robustness. The aforementioned publications require some auxiliary way of handling geometric degeneracies (*post-facto* checks on accuracy in the case of Dukowicz et al. 1991, and *ad-hoc* handling of all possible degenerate situations in the case of Grandy 1999). As discussed in Section 3.2, our clipping method is automatically robust and thus requires no such checks.

3. Algorithm

We now describe our voxelization algorithm in detail. Note that for our application, we have restricted the problem to voxelizing tetrahedra. However, the concepts can be easily extended into a conservative remesh operation between any meshes, as long as they consist of convex polyhedra.

The key idea in the voxelization process is to recognize that each intersection between an input tetrahedron and a voxel is itself a convex polyhedron whose volume and moments can be calculated using a simplicial decomposition.

This explanation can be made clearer by noting that there are really three types of voxels we must consider:

1. Voxels which lie completely inside of the input tetrahedron.
2. Voxels which lie completely outside of the input tetrahedron.
3. Voxels which cross the boundary of the input tetrahedron.

Types 1 and 2 are trivial to deal with. Voxels lying completely outside the tetrahedron can be ignored, and voxels lying completely inside can be integrated over analytically, since they are axis-aligned cubes. Type 3 is the core of the algorithm because it requires us to construct the polyhedral domain formed by the intersection of the voxel and the tetrahedron in a geometrically robust way, a nontrivial operation.

Hence, we break the algorithm into three main parts:

Searching is the operation of differentiating between the three voxel types; it amounts to efficiently finding voxels of type 3.

Clipping is the operation of taking a type 3 voxel and constructing the polyhedron resulting from its intersection with the input tetrahedron.

Reduction is the operation of computing the integral of a polynomial density field over voxels of types 1 and 3. Voxels of type 1 can be reduced trivially, as noted above. Clipped voxels of type 3 must be decomposed into simplices for computation of the integral. It is this last step that dominates the reduction operation, so for practical purposes, we use “reduction” to mean the combined process of simplicial decomposition and integration of clipped voxels.

3.1. Searching

We can differentiate between the types of voxels using the orientation of their vertices with respect to the faces of the tetrahedron. By “orientation,” we mean the signed distance from a vertex at position \mathbf{x} to the face labeled f ; e.g.

$$d_f = (\mathbf{x} - \mathbf{x}_f) \cdot \mathbf{n}_f \tag{3.1}$$

where \mathbf{n}_f is the unit normal of the face and \mathbf{x}_f is a point coplanar with the face. Points for which $d_f \leq 0$ are considered “behind” or “outside of” f , while points for which $d_f > 0$ are “inside” or “in front of” f .

Voxels with all eight vertices lying outside of the same face of the tetrahedron must be entirely excluded (type 1), and can be ignored. Likewise, voxels with all 8 vertices lying inside of all faces of the tetrahedron must be entirely included (type 2), and can be integrated over easily. Voxels that fall into neither of the above categories are close to the boundary of the tetrahedron (type 3), and must be clipped and reduced.

Testing vertices of the grid against the faces of the tetrahedron is a time-consuming operation, especially if the grid is fine.

In the most naïve implementation, we test each grid vertex against all four faces of the tetrahedron exactly once, storing the results in a buffer. The number of evaluations of (3.1) in this brute-force approach scales as $\mathcal{O}(g^3)$, where g is the linear dimension of the grid.

It is possible to do better using a binary space partitioning scheme. Instead of checking the vertices of individual voxels against the faces of the tetrahedron, we begin by checking the corner vertices of the entire target grid. We then split this box in two across the longest dimension and check the vertices of those children. This recursive splitting process continues until one of three things happens:

1. All eight vertices of the current box lie outside of the same face of the tetrahedron, so all enclosed voxels are completely outside of the tetrahedron. We stop recursing and ignore all voxels in the box.
2. All eight vertices of the current box lie inside of all faces of the tetrahedron, so all voxels in the box must be fully contained in the tetrahedron. We stop recursing and process all voxels in the box using a for-loop.
3. The current box contains a single voxel, which must lie on the boundary of the tetrahedron. We stop recursing, clip, and reduce the voxel.

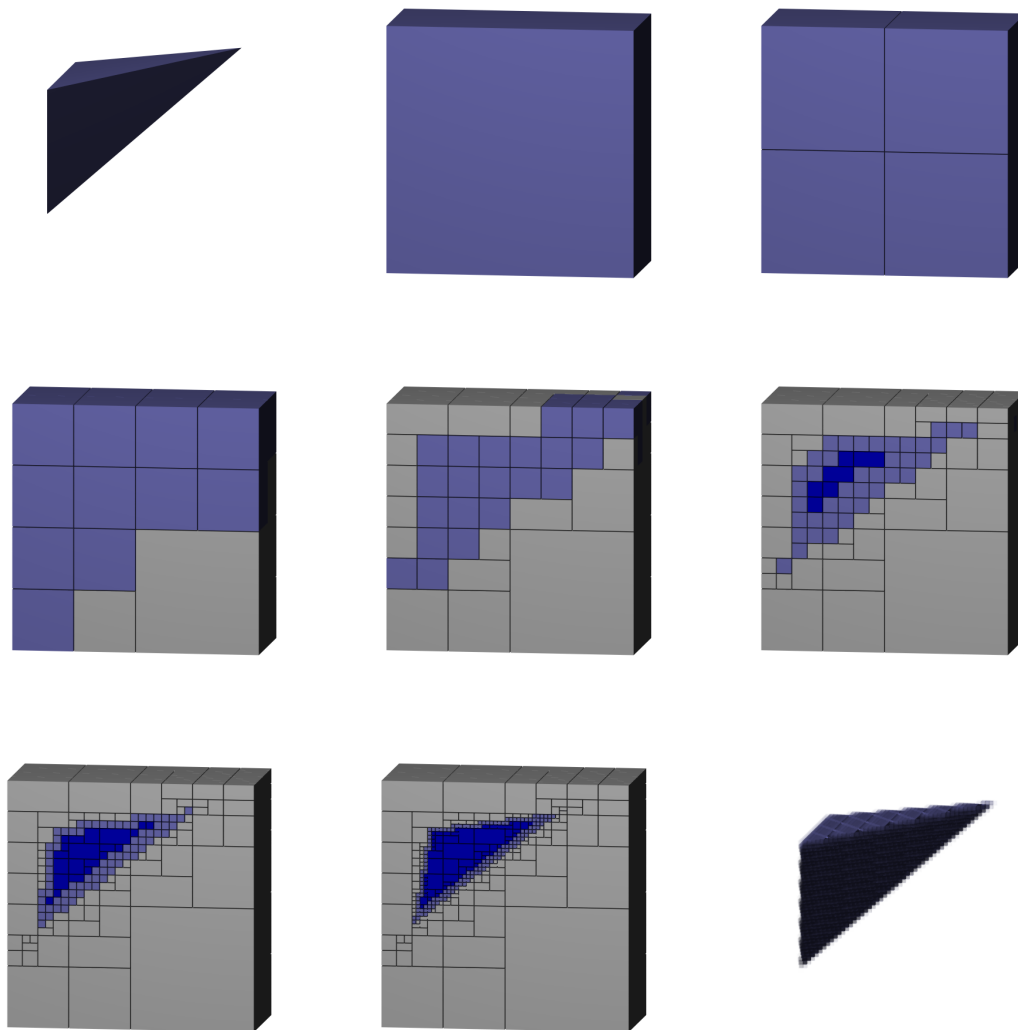


Figure 4: A binary space partitioning scheme for minimizing grid vertex orientation checks. Top left: An input tetrahedron to be voxelized. Top center to bottom center: Recursive refinement of grid regions. Corners of the grid are checked for inclusion in the tetrahedron. Regions that lie entirely outside of the tetrahedron (gray) can be ignored, whereas regions that are entirely included (dark blue) can be integrated over easily using a for-loop. Regions whose inclusion is ambiguous (light blue) must lie near the boundary, and are recursively split until they contain a single voxel. Bottom right: The voxelized tetrahedron.

Figure 4 gives an illustration of this binary partitioning process.

The number of vertex checks in this binary partitioning approach scales as $\mathcal{O}(g^2 \log g)$. This is better in principle than the brute-force approach; however, the added overhead of keeping track of a stack of tree nodes means that practically speaking, the brute-force approach does better when the target grid is coarse. We discuss this further in the results section.

3.2. Clipping

Any voxels found to lie across the boundary of the tetrahedron must be clipped against the faces of the tetrahedron, so that the polyhedron resulting from the intersection of the voxel and the tetrahedron can be known explicitly. By “clipping” we mean “truncation”: we are finding the intersection of a polyhedron with a half-space (the volume of the original polyhedron that is “in front of the clip plane”), throwing away vertices lying outside of the half space (“behind the clip plane”), and inserting new vertices along edges bisected by the clip plane.

We accomplish this through a directed graph traversal. By Steinitz’s theorem (Steinitz 1922), any convex polyhedron can be represented as a three-vertex-connected planar graph (sometimes called a polyhedral graph for this reason) whose vertices and edges are isomorphic to those of the polyhedron. We use this theorem to our benefit by representing polyhedra using their graphs, in a modification of the well-known “half-edge” or “doubly-connected edge list” representation for polyhedra. This one-skeleton of the polyhedron provides us with all the necessary information for the geometric operations described here. The basic idea of using this representation for robust clipping is reported by Sugihara (1994), though the algorithm is described rather abstractly. We give a concrete implementation which uses a graph traversal over the polyhedron itself.

The problem of clipping a polyhedron against a plane then reduces to finding the connected component of its graph whose vertices lie behind the clip plane.

We store polyhedra as triply-linked sets of vertices, where each vertex consists of a coordinate for its spatial location, three pointers to its neighboring vertices, a byte used to indicate whether the vertex has been clipped, and four floating-point numbers giving the signed distance to each clip plane. Although each vertex this data structure is formally adjacent to three edges, we can effectively represent an arbitrary number of edges per vertex by employing spatially degenerate vertices connected by edges of zero length; this feature is essential for geometric robustness. Faces are represented implicitly, as loops in the planar graph naturally give us vertices in the proper order around each face.

The algorithm is as follows. First, the graph of the initial cubical voxel is initialized. We then traverse the graph using a depth-first search. We begin by finding a vertex behind the clip plane, simply looping over existing vertices until one is found (this is fast, as the floating-point operations involved have been previously evaluated). If we cannot find a starting vertex, we have determined that the entire polyhedron lies in front of the clip plane, and so will be unaffected. Otherwise, we start at this vertex and begin traversing the graph. Vertices visited in the traversal are marked as clipped and ignored hereafter.

Each time a vertex is visited which is in front of the clip plane, we calculate the intersection point between the clip plane and the edge formed by the current and previous vertices (see Section 4.1 for further explanation). A new vertex is assigned the correct position, its signed distance to each remaining clip plane is calculated, and it is inserted into the graph. The previous vertex is marked as having been clipped.

When the traversal ends (all edges behind or crossing the clip plane have been visited), we have in hand an explicit representation of the clipped voxel, with no need to reconstruct the vertex ordering. We then repeat the process for each remaining face of the input tetrahedron.

An illustration of the edge traversal process for clipping is given in Figure 5.

Approaching the clipping operation in this way has two major benefits:

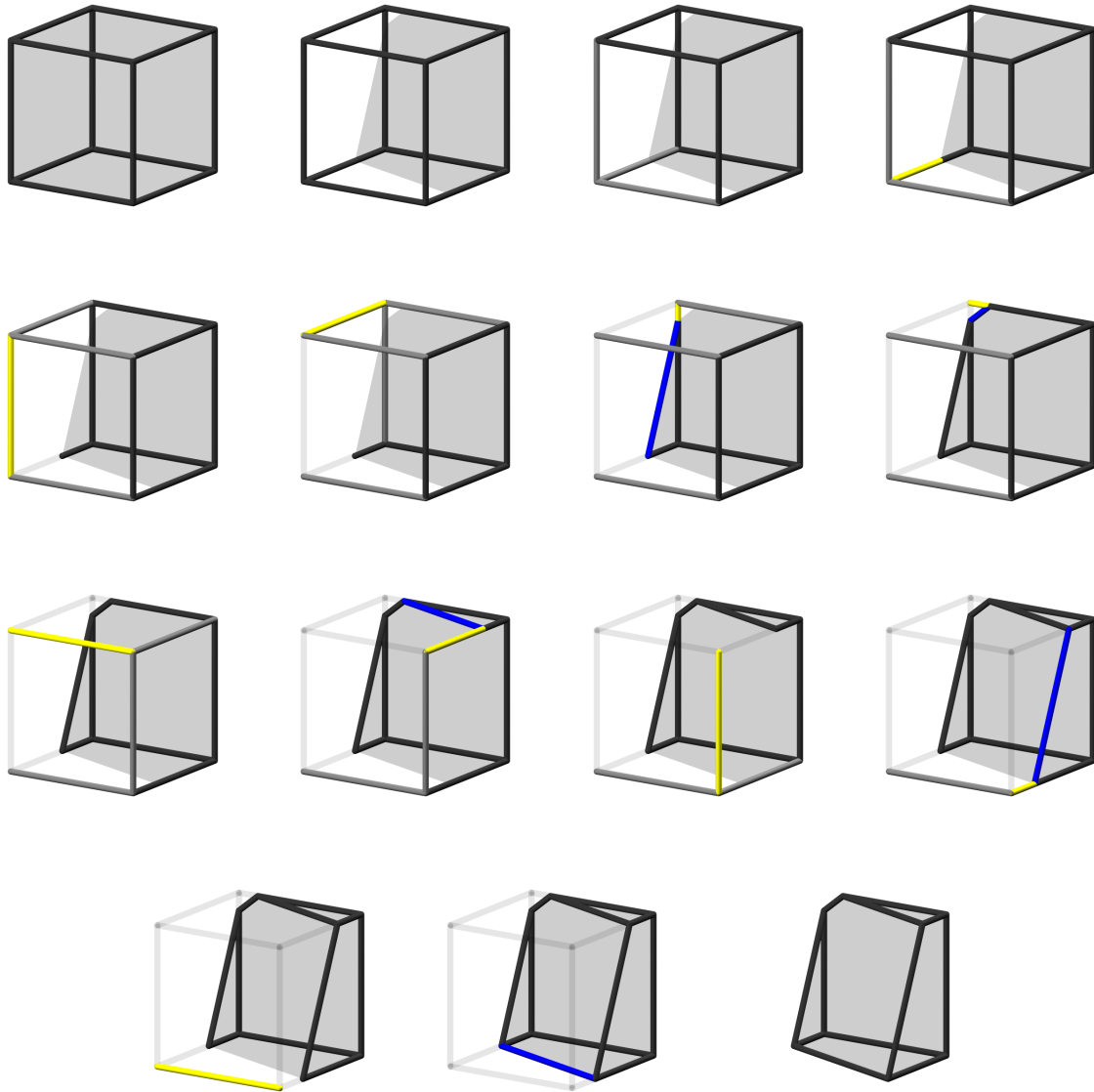


Figure 5: Traversal of edges in a voxel for clipping against a plane while automatically building connectivity of the resulting polyhedron. Top left: The input voxel. Top, second from left: The shaded region indicates the location of the clip plane. Remaining panels: The planar graph formed by the vertices and edges of the voxel is traversed. Each time the working edge (yellow) is bisected by the clip plane, a new edge (blue) is inserted. The working edge makes its way around the clip plane in an ordered fashion, so that new edges and vertices are automatically inserted with the appropriate connectivity. Bottom right: The clipped voxel.

1. We recover new vertices in the correct order (e.g., clockwise around the clip face) due to the directed nature of the depth-first graph traversal. This allows us to insert new vertices on the fly by implicitly knowing the connectivity to neighboring vertices, which

saves us from having to reconstruct the polyhedron after each clip operation. As we show in Section 5, this provides substantial performance gains over previous methods.

2. We ensure that the geometrical information in the output is complete and consistent. In graph-theoretical terms, we always guarantee preservation of the planar, three-vertex-connected nature of the graph while inserting and removing vertices during the clipping process. This makes our algorithm robust to degenerate geometry.

3.3. Reduction

Once we have finished clipping a voxel, we are ready to calculate the integral of the input density over the clipped voxel. We do this using a simplicial decomposition, e.g. we represent the clipped voxel as the union of a set of tetrahedra, so that the total integral can be found by summing the integrals over each tetrahedron.

The decomposition is also based on a directed graph traversal over the edges. We construct faces on the fly using the fact that loops in the graph are a natural representation for the faces of the polyhedron. Because the clipping process is robust, we can assume that vertices on a loop are coplanar. So, each time we process a new face, we save the first vertex and then loop around the edges. Each edge, the starting vertex, and the origin form a fan of tetrahedra. It is over each of these tetrahedra that we integrate before finally summing the results over the entire decomposition. See Figure 6 for an illustration of the clipping and reduction process.

One vertex of every tetrahedron in the decomposition is fixed at the origin, to eliminate several floating-point operations. Due to the linearity of the integrals and the orientation of the tetrahedra, the sum is always correct, even if the origin lies outside of the original clipped voxel.

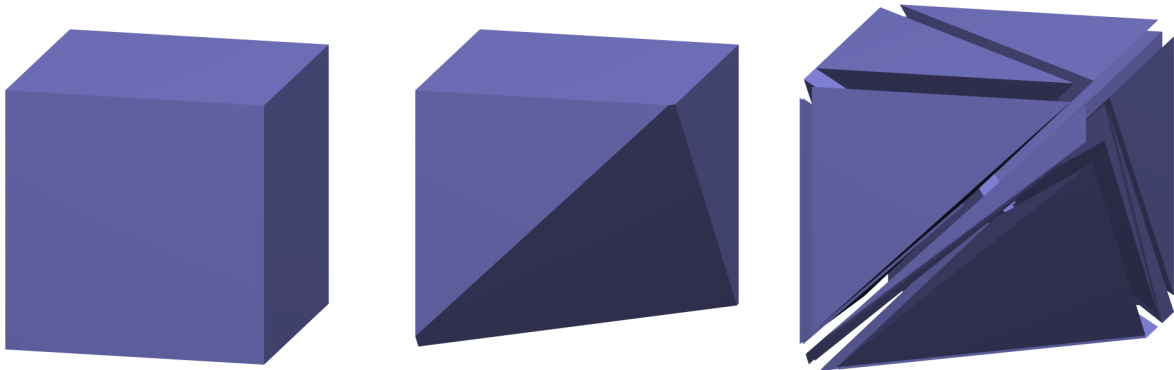


Figure 6: An illustrated summary of our method. Left: An initial cubical voxel. Middle: The voxel, clipped against faces of a tetrahedron, giving a convex polyhedral domain over which we must integrate. Right: The clipped voxel, decomposed into simplices for integration.

Now we discuss the integration itself. The volume of a tetrahedron is given in terms of the vertex coordinates by the determinant

$$V = \frac{1}{6} \begin{vmatrix} 1 & 1 & 1 & 1 \\ x_0 & x_1 & x_2 & x_3 \\ y_0 & y_1 & y_2 & y_3 \\ z_0 & z_1 & z_2 & z_3 \end{vmatrix} \quad (3.2)$$

The integral of a polynomial over a tetrahedral domain Ω_t has been well-known in the finite element community for some time. Eisenberg and Malvern (1973) give a proof for the following formula:

$$\int_{\Omega_t} \zeta_0^a \zeta_1^b \zeta_2^c \zeta_3^d d\Omega_t = 6V \frac{a! b! c! d!}{(a + b + c + d + 3)!} \quad (3.3)$$

where ζ_i are the barycentric coordinates, a , b , c , and d are integer exponents, and V is the volume of the tetrahedron (found using (3.2)).

Because the integral is given in terms of the barycentric coordinates, we must express it in terms of Cartesian coordinates. We make use of the fact that

$$\mathbf{x} = \mathbf{x}_0 \zeta_0 + \mathbf{x}_1 \zeta_1 + \mathbf{x}_2 \zeta_2 + \mathbf{x}_3 \zeta_3$$

where \mathbf{x}_i are the vertex coordinates of the tetrahedron. This allows us to explicitly evaluate an integral expressed in Cartesian coordinates by substituting the above relation. For example,

$$\begin{aligned} \int_{\Omega_t} x^2 d\Omega_t &= \int_{\Omega_t} (x_0 \zeta_0 + x_1 \zeta_1 + x_2 \zeta_2 + x_3 \zeta_3)^2 d\Omega_t \\ &= \frac{V}{10} (x_0^2 + x_1^2 + x_2^2 + x_3^2 + x_0 x_1 + x_0 x_2 + x_0 x_3 + x_1 x_2 + x_1 x_3 + x_2 x_3) \end{aligned}$$

In the case where we allow x_0 to lie at the origin, we can simplify further to

$$\int_{\Omega_t} x^2 d\Omega_t = \frac{V}{10} (x_1^2 + x_2^2 + x_3^2 + x_1 x_2 + x_1 x_3 + x_2 x_3)$$

This recipe is the same for all coordinate moments (see Section 4.3).

4. Practical considerations

4.1. Calculation of new vertex locations

We use a weighted averaging procedure to calculate the positions of new vertices.

Consider two vertices \mathbf{x}_0 and \mathbf{x}_1 that form the endpoints of an edge that is bisected by a clip plane. In other words, let \mathbf{x}_0 lie in front of the plane, so that its signed distance to the plane $d_0 > 0$. Let \mathbf{x}_1 lie behind the plane, so that its signed distance to the plane $d_1 \leq 0$. We can calculate the point of intersection \mathbf{x}_p between the edge and the plane as

$$\mathbf{x}_p = \frac{d_0 \mathbf{x}_1 - d_1 \mathbf{x}_0}{d_0 - d_1} \quad (4.1)$$

Due to strict use of inequalities in the clipping routine, we guarantee the denominator $d_0 - d_1 > 0$ even in finite precision, so we are automatically protected from divide-by-zero errors.

The main advantage to using this approach is that it is numerically far more stable than calculating the intersection point using the plane and the edge in parametric form, especially when \mathbf{x}_0 , \mathbf{x}_1 , or both, lie very near to the plane. Even if \mathbf{x}_0 and \mathbf{x}_1 are nearly coplanar, the resulting vertex will lie between the two.

A similar weighted averaging approach is used to calculate the signed distance from the new vertex \mathbf{x}_p to each of the remaining faces. So, once we find the signed distance to each vertex of a voxel pre-clipping, there is no need to further keep track of any additional information regarding the faces.

4.2. Cancellation error

We note that calculating volumes and moments using simplicial decomposition (see Section 3.3) can give rise to cancellation errors when evaluated on a computer.

Consider a tetrahedron whose vertices lie in the box $(x - \Delta x, x - \Delta x, x - \Delta x)$, (x, x, x) , where $|\Delta x| < |x|$ (this is a worst-case example in which all coordinates are larger than the size of the tetrahedron). The volume calculation $V \sim \mathcal{O}(\Delta x^3)$ using (3.2) involves the subtraction of terms of order $\mathcal{O}(x^3 - \Delta x^3)$ from terms of order $\mathcal{O}(x^3)$.

We can estimate the error due to cancellation as follows. b , the number of significant bits lost during subtraction, is approximately

$$\begin{aligned} 2^{-b} &\approx 1 - \frac{(x^3 - \Delta x^3)}{x^3} \\ &\approx \left(\frac{\Delta x}{x}\right)^3 \end{aligned}$$

The fractional error $E \approx 2^{b-p}$ is then dependent on the number of bits p in the significand ($p = 53$ in double precision and $p = 24$ in single precision for the IEEE floating-point standard):

$$E \approx 2^{-p} \left(\frac{\Delta x}{x}\right)^{-3} \quad (4.2)$$

This is a toy calculation, and errors will obviously be dependent on the exact geometry in question, so (4.2) serves as a rough estimate of how errors should scale with $\Delta x/x$, the size of the integration domain relative to its absolute coordinate position.

Because of this error scaling, it is beneficial to shift the domain into a local coordinate system near the origin prior to performing the calculation. In our implementation, we process each voxel with its center lying at the origin.

In shifting the domain, cancellation errors are still unavoidable. However, doing so changes the scaling of errors in a way that is more acceptable. Following the same logic as before, subtracting a coordinate offset *prior* to calculating the volume and moments gives the following error scaling:

$$E \approx 2^{-p} \left(\frac{\Delta x}{x}\right)^{-1} \quad (4.3)$$

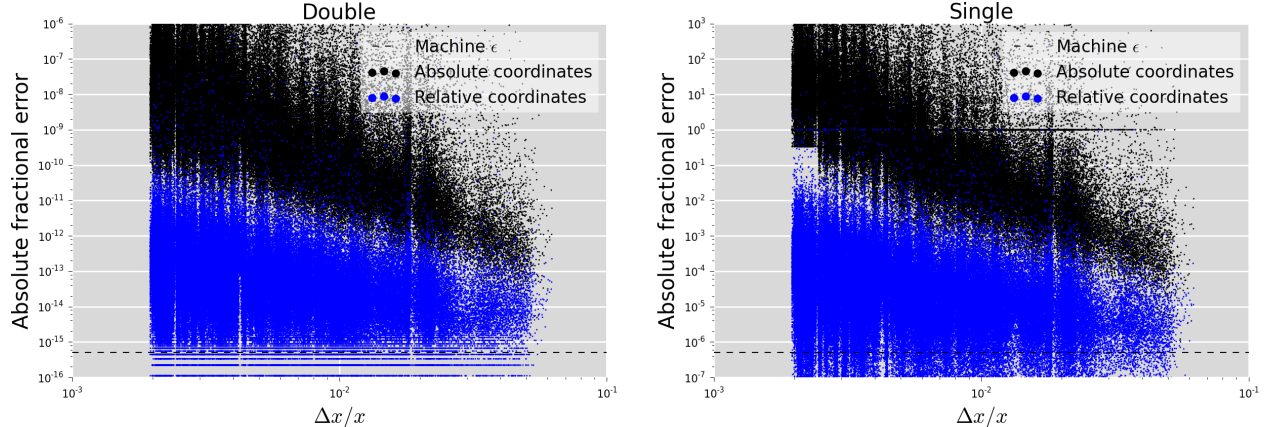


Figure 7: Reducing cancellation errors by calculating the volume of each clipped voxel in a relative coordinate frame centered on the origin, for double- (left) and single-precision (right) calculations. This demonstration was done on a sample of 1.9×10^5 clipped voxels extracted from 100 pseudo-randomly generated tetrahedra on a 512^3 grid. Calculations were validated against the quadruple-precision solution. Errors are much more well-behaved when we calculate the volume in a relative coordinate frame near the origin.

Now, cancellation errors scale linearly with $x/\Delta x$ rather than cubically. So, while some cancellation errors are unavoidable due to the nature of the problem, we are able to reduce their effect substantially. Figure 7 shows this scaling for both single- and double-precision calculations. We indeed see that calculating the volume and moments in a relative coordinate system near the origin is essential to the overall accuracy of our method.

For higher-order moments, such a coordinate translation gives rise to cross terms that must be taken into account later, but involve only addition and thus do not contribute to cancellation errors. For example, the calculation of the first moment in x over a voxel whose center lies at x_0 means first evaluating the moment as though the voxel were centered on the origin, then adding back in a correction for this coordinate offset:

$$\int_V x \, dV = \int_V (x - x_0) \, dV + x_0 V$$

We note that while this use of a relative coordinate system greatly reduces cancellation errors, any other numerical error in the calculation of the volume V in the above expression will be scaled by a factor of x_0 and propagated into the final result. The same applies to cross-terms arising in the evaluation of higher-order moments. This is unavoidable.

We present full results concerning the accuracy of our method in Section 5.3.

4.3. Moments

Our implementation of this method consists of using the algorithm described above to first find coordinate moments over each voxel, then taking linear combinations of these moments using polynomial coefficients. This allows the simultaneous integration of an arbitrary number of scalar fields (or component-wise integration of vector fields) with no need to re-clip voxels.

For example, consider the integral of the second-order polynomial field

$$\int_V (Ax^2 + By^2 + Cz^2 + Dxy + Exz + Fyz + Gx + Hy + Iz + J) dV$$

Given the representation of this field in terms of the constant coefficients $A \cdots J$, finding the integral of the field amounts to finding the integral over each of the coordinate moments

$$\int_V x^2 dV \cdots \int_V xy dV \cdots \int_V x dV \cdots V$$

Once all moments for the desired polynomial order are evaluated, any further manipulation (gradient estimation, field normalization, etc.) becomes a linear algebra problem in the space of polynomial coefficients.

4.4. 2D

All of the concepts presented above extend trivially to two dimensions. The graph traversals in the clipping and reduction operations simplify greatly, since the topology of a polygon is a loop.

As a demonstration, we perform a conservative remesh in 2D. We begin with a uniform, Cartesian grid of unit-density quadrilaterals. We then deform the grid by displacing the gridpoints according to the transformation (in polar coordinates relative to the center of the grid):

$$\begin{aligned} r &\rightarrow r S(r/r_0) \\ \theta &\rightarrow \theta + T(r/r_0) \end{aligned}$$

where

$$S(x) = \begin{cases} 1 - S_0(x-1)^2 & 0 \leq x < 1 \\ 0 & x \geq 1 \end{cases}$$

and

$$T(x) = \begin{cases} T_0(x^2-1)^2 & 0 \leq x < 1 \\ 0 & x \geq 1 \end{cases}$$

We use the constants $r_0 = 0.45$ (on a grid of side length 1.0), $S_0 = 0.2$, and $T_0 = \pi/2$. The analytic density $\rho(r/r_0)$ resulting from this Lagrangian deformation is given by

$$\rho(x) = \begin{cases} \frac{1}{(S_0(x-1)^2-1)(S_0(3x^2-4x+1)-1)} & 0 \leq x < 1 \\ 1 & x \geq 1 \end{cases}$$

We then remesh this deformed grid back onto the original Cartesian grid. Figure 8 illustrates this deformation and remesh process. Total mass is conserved to machine precision. Note that near the boundaries, the old and new meshes are exactly degenerate (lie exactly on top of) one another. This demonstrates the geometrical robustness of our method.

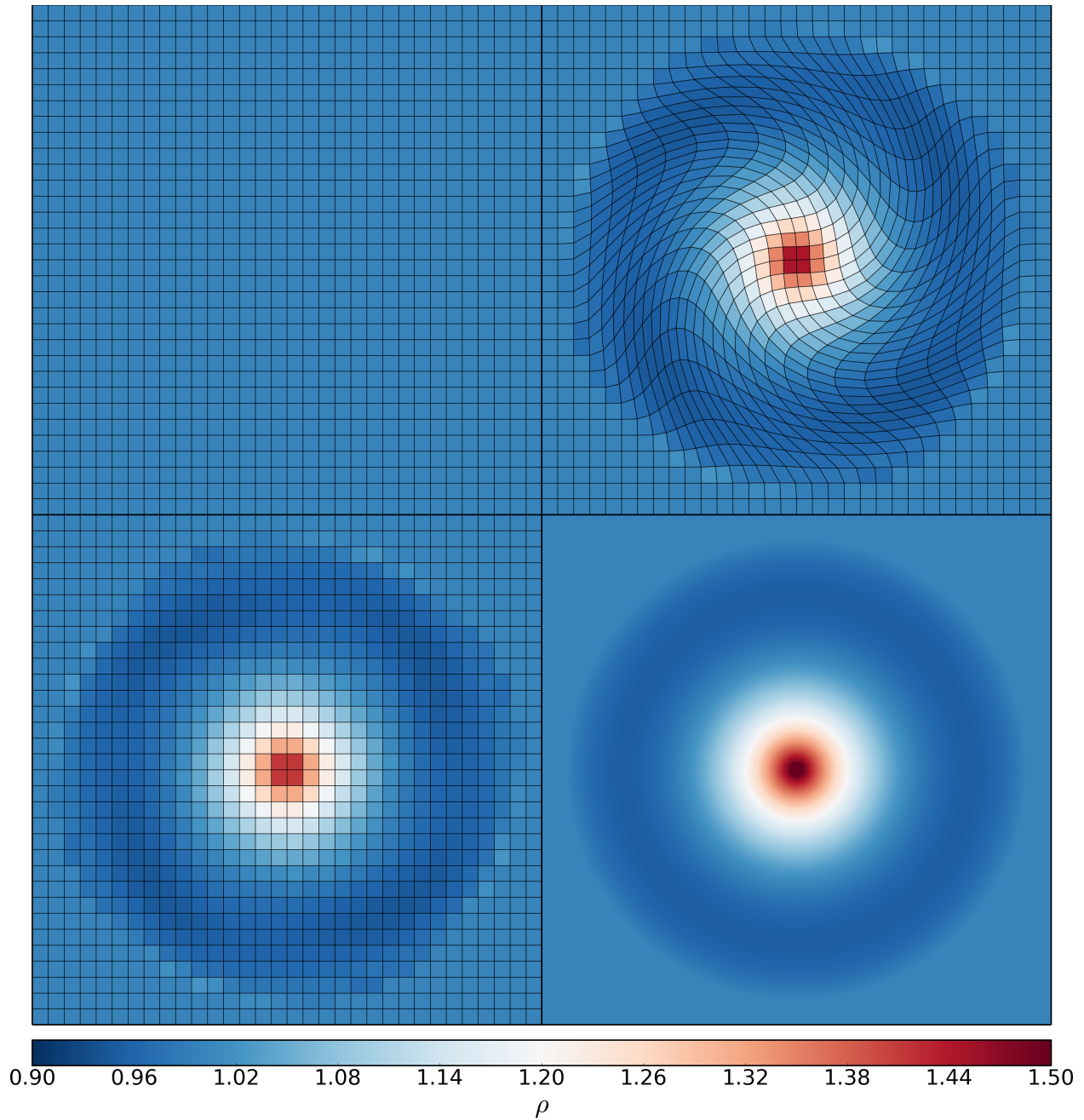


Figure 8: A conservative remesh between quadrilateral grids in 2D. Top left: The initial grid, with constant unit density. Top right: The grid, deformed by displacing vertices according to the Lagrangian deformation described in Section 4.4. This deformation creates a varying density field. Bottom left: The resulting density field, remeshed onto the original grid. Bottom right: The analytic density for the Lagrangian transformation used.

5. Results and Discussion

In this section, we present the results of numerical tests of our C implementation of this work (available at <https://github.com/devonmpowell/r3d>). We first compare results

for isolated clipping and reduction operations against previous work, to give a sense of performance as a general remesh scheme. We then move on to overall accuracy, timing, and robustness results for voxelizing tetrahedra.

For fairness in comparisons, we always bring the polyhedron into the appropriate representation for a method (e.g., planar graph vs. explicit face-vertex connectivity) separately from the operation being timed.

All tests in this section were compiled using `gcc`, `g++`, and `gfortran` using full optimizations (`-O3`), and run on a 2.2GHz Intel Xeon E5-2660 processor. Unless otherwise stated, double-precision arithmetic was used in all computations.

5.1. Clipping

We compare our method to the clipping algorithm by Stephenson and Christiansen (1975), as implemented in Fortran by López and Hernández (2008) as a part of their VOFTools software. This software also includes a function for calculating volumes of polyhedra using the expression

$$V = \frac{1}{6} \left[\sum_{j=1}^J (\mathbf{n}_j \cdot \mathbf{x}_{j,1}) \mathbf{n}_j \cdot \sum_{i=1}^{I_j} (\mathbf{x}_{j,i} \times \mathbf{x}_{j,i+1}) \right]$$

where \mathbf{n}_j is the unit normal of the j^{th} face and $\mathbf{x}_{j,i}$ is the i^{th} vertex around face j . We compare the speed of this volume computation as well. A fuller comparison of speed and accuracy for the reduction process, including computation of all coordinate moments up to second order, is given in the next section.

For this comparison, we clipped a unit cube against a successively increasing number (1, 2, 3, and 4) of planes. For each test, we timed 10^6 iterations. The results are summarized in Table 1. Our calculation of volumes using simplicial decomposition by traversing the planar graph is slightly slower than the above expression used by López and Hernández (2008). However, the speed of our clipping operation is faster by a factor of 3-4. This is due to the fact that we are able to insert new vertices on the fly with the correct ordering, whereas López and Hernández (2008) must post-process the clipped polyhedron to bring new vertices into the correct order.

5.2. Reduction

We now show a comparison of our reduction process with three other methods. The first is a control consisting of the same simplicial decomposition scheme used here, but implemented using for-loops rather than the planar graph traversal (the decomposition scheme is the same, though ordering of operations may vary). The second is the volume computation given by López and Hernández (2008). The third is the volume and moments computation using dimensionality reduction, by Mirtich (1996).

We computed volumes and moments for three polyhedra of varying complexity: a tetrahedron, a cube, and a dodecahedron, all scaled and translated to lie in the unit cube in the first octant. For each test, we ran 10^6 iterations. Errors were calculated relative to the solution of Mirtich (1996). We show results for both timing and accuracy in Table 2.

Our reduction using a graph traversal carries a slight overhead compared with the for-loop implementation and López and Hernández (2008), though this overhead becomes much less

Clip planes	This work		López and Hernández (2008)	
	Clip (ms)	Clip & reduce (ms)	Clip (ms)	Clip & reduce (ms)
0	-	280	-	180
1	220	580	870	1080
2	370	790	1360	1620
3	560	1050	1920	2200
4	760	1320	2550	2880

Table 1: Comparison of timing with the clipping and volume implementations of López and Hernández (2008). A cube was clipped against different numbers of planes. Times are given in milliseconds per 10^6 trials. Although the volume computation is slower in our implementation due to overhead in the graph traversal, our representation of the polyhedron as a planar graph gives an overall speed-up, as it automatically inserts new vertices in the proper order.

	This work			Decomposition, for-loop		
	Volume (ms)	Moments (ms)	Error	Volume (ms)	Moments (ms)	Error
Tetra.	150	290	7.2×10^{-16}	60	220	7.2×10^{-16}
Cube	280	670	1.7×10^{-16}	170	610	1.7×10^{-16}
Dodec.	690	1850	9.2×10^{-16}	500	1820	7.3×10^{-16}

	López and Hernández (2008)			Mirtich (1996)		
	Volume (ms)	Moments (ms)	Error	Volume (ms)	Moments (ms)	Error
Tetra.	100	-	3.3×10^{-16}	-	1050	0.0
Cube	180	-	0.0	-	1760	0.0
Dodec.	400	-	0.0	-	3980	0.0

Table 2: Comparison of timing and accuracy between reduction methods. Times are given in milliseconds per 10^6 trials. The error quoted is the maximum absolute fractional error from all 10 coordinate moments, except for López and Hernández (2008), where only volume information is available. We see that reduction using our graph traversal is slightly slower, though this becomes less significant when higher-order moments are calculated.

significant when higher-order moments are calculated, due to the dominance of floating-point operations in the computation. All calculations agree to within machine precision.

5.3. Full voxelization results

To test the overall accuracy of our method in terms of conservation, we voxelized 10^5 tetrahedra of unit density whose vertices were randomly chosen to lie in the unit cube onto

a 128^3 grid. This gave a volume of 1.3×10^{-2} , 2.3×10^4 interior (type 1) voxels, and 1.5×10^4 boundary (type 3) voxels requiring clipping, per tetrahedron on average. We compare the rms and maximum fractional errors between the moment integrals of the input tetrahedron and the sum over all voxels in the output. The results are summarized in Table 3.

	Double		Single	
	rms	max	rms	max
Constant	1.7×10^{-12}	5.2×10^{-10}	5.6×10^{-4}	1.4×10^{-1}
Linear	1.6×10^{-12}	5.4×10^{-10}	5.4×10^{-4}	1.7×10^{-1}
Quadratic	1.6×10^{-12}	5.7×10^{-10}	5.3×10^{-4}	1.9×10^{-1}

Table 3: Accuracy (conservativeness) of our voxelization method in double- and single-precision, for a sample of 10^5 randomly-generated tetrahedra on a 128^3 grid. Here we quote the maximum fractional error between the pre- and post- voxelization moments. Errors for each polynomial order are taken from all moments in that order (e.g. “linear” includes x , y , and z moments).

We see that, although quite accurate, we are still a few orders of magnitude in accuracy away from machine precision, even though the reduction process itself is accurate to machine precision (see Section 5.2). This is due to the unavoidable presence of cancellation errors that arise in shifting each voxel to a local coordinate frame prior to integration. See Section 4.2 for a full discussion of these errors.

To demonstrate the geometrical robustness of our method, we repeated the same test as before; however, this time we randomly generated the tetrahedron vertices at integer multiples of the grid spacing. This ensures that we have exactly degenerate geometry. The results are shown in Table 4.

	Double		Single	
	rms	max	rms	max
Constant	5.6×10^{-14}	7.2×10^{-14}	3.3×10^{-5}	6.0×10^{-3}
Linear	5.8×10^{-14}	7.5×10^{-14}	3.4×10^{-5}	6.7×10^{-3}
Quadratic	6.1×10^{-14}	8.1×10^{-14}	3.5×10^{-5}	7.7×10^{-3}

Table 4: The same accuracy test as Table 3, but for tetrahedra whose vertices were chosen to be exactly degenerate with the grid. Our method is immune to such geometrical degeneracies, as demonstrated by the high accuracy of the computations.

The results indicate that the degenerate case is actually *more* accurate than the general case. This is due to the fact that we ran this test on a 128^3 grid, a power of two, to ensure exact geometric degeneracies in the binary representation. A side effect is that the computations themselves are more accurate, since they take place in a representation that favors binary fractions of the grid spacing. So, the numbers in Table 4 should not be taken as a statement about the general accuracy of the code (for that, refer to Table 3), but as a statement of the geometric robustness of our method.

As a final test, we check the performance scaling of the voxelization routine with grid resolution. We repeat the same test as before (10^5 tetrahedra with randomly generated, though nondegenerate, vertices), voxelizing them onto grids of increasing linear resolution g , up to 1024^3 . We do this for both search methods described in Section 3.1 (brute-force and binary space partitioning). The results are summarized in Figure 9.

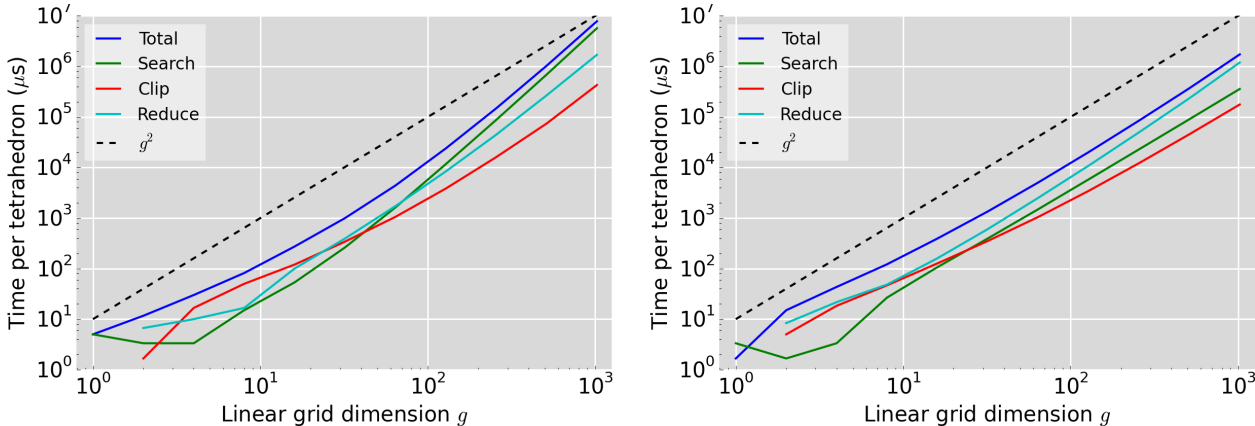


Figure 9: Timing of the operations involved in our voxelization method. In both cases, the clip and reduce operations scale roughly quadratically in the grid dimension (e.g. linearly with surface area), as expected. Left: Using a full grid buffer to search for voxels that need further processing makes the search operation scale as the cube of the grid dimension. Right: Spatial tree for voxel searching. All operations scale quadratically in the grid dimension (the search operation contains a logarithmic component, but the quadratic term dominates). The reduction operation also does slightly better, since large blocks of fully included voxels can be processed together.

We see that, in general, the performance scales as g^2 , or equivalently, as the effective surface area of the tetrahedra in units of squared grid spacing. This is consistent with our expectations, since clipping and reduction are the most costly operations involved, and they take place only on the boundaries of tetrahedra. An exception to this scaling arises in the brute-force search method, which checks every grid point against each tetrahedron face, and so scales as g^3 when the grid becomes sufficiently fine. This is in contrast to the binary space partitioning search, which scales as $g^2 \log g$. However, in practical terms, the brute-force method actually performs better for coarser grids due to the added overhead of the binary search. Binary partitioning only overtakes brute-force at a grid resolution of 128^3 , corresponding to an average tetrahedron volume of $\sim 3 \times 10^4$ voxels.

6. Conclusion

We describe a general remeshing method, in that we present an approach to robustly intersecting two convex polyhedra and computing a polynomial integral over the resulting intersection domain.

Such an operation is useful for computational physics in several areas. These include ALE and re-ALE hydrodynamics, in which fluid quantities must be transferred between meshes

in a geometrically precise way, sometimes with higher-order polynomial interpolation (e.g. Donea et al. 2004, Loubère et al. 2010, Dukowicz and Kodis 1987, and Dukowicz et al. 1991). Interface reconstruction and volume-of-fluid methods (Hirt and Nichols 1981, Renardy et al. 2001, López and Hernández 2008) also rely on such a geometric intersection followed by an integral. Computing exact integrals over the intersection between two polyhedra is also useful in computer graphics and visualization, where the exact computation of convolution integrals is of interest (e.g. Catmull 1978, Duff 1989, Auzinger et al. 2012, and Auzinger and Wimmer 2013). We focus on yet another application, the exact mass-conservative voxelization of tetrahedra for the simulation and analysis of cosmological N -body systems using the approach of Abel et al. (2012). This interpretation of the N -body problem has proven quite useful in recent work (Kaehler et al. 2012, Hahn et al. 2013, Angulo et al. 2014, Hahn et al. 2014).

This general problem of computing exact intersection volumes between polyhedra and integrating over those volumes has been studied in detail by Dukowicz and Kodis (1987), Dukowicz et al. (1991), and Grandy (1999). Additionally, López and Hernández (2008) give an implementation of the basic clipping operation of Stephenson and Christiansen (1975). A common issue that these implementations must deal with is how to handle geometric degeneracies in the input. For example, Dukowicz et al. 1991 impose *post-facto* checks on accuracy, while Grandy 1999 employs *ad-hoc* handling of all possible degenerate situations.

The main contribution of this paper is to put forth a unified framework for the problem of intersecting convex polyhedra in a geometrically robust way, and subsequently computing an integral over the resulting domain. The specific case on which we focus is the physically conservative voxelization of tetrahedra with polynomial densities. We present a C implementation as well.

Our algorithm for intersecting two convex polyhedra by successively clipping one against the faces of the other is based on the ideas of Sugihara (1994), who describes in abstract terms how the planar graph representation of a polyhedron can be used in a geometrically robust clipping algorithm by guaranteeing the topological validity of the output. Our implementation is based on a depth-first graph traversal, which ensures that it is automatically geometrically robust, with no need for auxiliary checks or high precision arithmetic. We couple the clipping algorithm to an integration routine on the same planar graph representation. As a result, we are able to store polyhedra using only vertex locations and neighbors, with no need for face normals.

We address practical issues including numerical stability of geometric calculations, management of cancellations errors, and extension to two dimensions. In a comparison to the implementation of López and Hernández (2008), we show that our clipping operation is faster by a factor of 3-4, with an overall speed-up by a factor of 2. This is due to the algorithm's ability to insert new vertices in the correct order on the fly, with no need to reorder them post-clipping. Our implementation conserves the integral between the input and output meshes to high precision.

Our C code (available at <https://github.com/devonmpowell/r3d>) is intended to be a simple tool for carrying out fast, accurate, and robust geometrical calculations on the convex polyhedral mesh elements often used in computational physics.

Acknowledgements

We are grateful to T. Sousby and O. Hahn for useful discussions on this topic. T.A. also is grateful Pat Hanrahan for suggesting some classic references and encouragement. We are indebted to R. Kaehler from whom we have learned a great deal about algorithms, rasterization, and GPUs.

D. Powell was supported in this work by the Fletcher Jones Foundation Stanford Graduate Fellowship. This work was also supported in part by the U.S. Department of Energy contract to SLAC no. DE-AC02-76SF00515.

References

- Abel, T., O. Hahn, and R. Kaehler (2012, November). Tracing the dark matter sheet in phase space. *MNRAS* 427, 61–76.
- Almgren, A. S., J. B. Bell, M. J. Lijewski, Z. Lukić, and E. Van Andel (2013, March). Nyx: A Massively Parallel AMR Code for Computational Cosmology. *ApJ* 765, 39.
- Anderson, R. W., V. A. Dobrev, T. V. Kolev, and R. N. Rieben (2015). Monotonicity in high-order curvilinear finite element arbitrary lagrangian–eulerian remap. *International Journal for Numerical Methods in Fluids* 77(5), 249–273.
- Angulo, R. E., R. Chen, S. Hilbert, and T. Abel (2014, November). Towards noiseless gravitational lensing simulations. *M.N.R.A.S.* 444, 2925–2937.
- Auzinger, T., M. Guthe, and S. Jeschke (2012, May). Analytic anti-aliasing of linear functions on polytopes. *Comp. Graph. Forum* 31(2pt1), 335–344.
- Auzinger, T. and M. Wimmer (2013). Sampled and analytic rasterization. In M. M. Bronstein, J. Favre, and K. Hormann (Eds.), *VMV*, pp. 223–224. Eurographics Association.
- Bockman, S. F. (1989, February). Generalizing the formula for areas of polygons to moments. *Am. Math. Monthly* 96(2), 131–132.
- Bruderlin, B. (1991, Jan). Robust regularized set operations on polyhedra. In *System Sciences, 1991. Proceedings of the Twenty-Fourth Annual Hawaii International Conference on*, Volume i, pp. 691–700 vol.1.
- Bryan, G. L., M. L. Norman, B. W. O’Shea, T. Abel, J. H. Wise, M. J. Turk, D. R. Reynolds, D. C. Collins, P. Wang, S. W. Skillman, B. Smith, R. P. Harkness, J. Bordner, J.-h. Kim, M. Kuhlen, H. Xu, N. Goldbaum, C. Hummels, A. G. Kritsuk, E. Tasker, S. Skory, C. M. Simpson, O. Hahn, J. S. Oishi, G. C. So, F. Zhao, R. Cen, Y. Li, and Enzo Collaboration (2014, April). ENZO: An Adaptive Mesh Refinement Code for Astrophysics. *ApJS* 211, 19.
- Catmull, E. (1978, August). A hidden-surface algorithm with anti-aliasing. *SIGGRAPH Comput. Graph.* 12(3), 6–11.
- De Loera, J., B. Dutra, M. Koeppe, S. Moreinis, G. Pinto, and J. Wu (2011, July). Software for Exact Integration of Polynomials over Polyhedra. *ArXiv e-prints*.
- Donea, J., A. Huerta, J.-P. Ponthot, and A. Rodríguez-Ferran (2004). Arbitrary lagrangian–eulerian methods. In *Encyclopedia of Computational Mechanics*. John Wiley and Sons, Ltd.
- Duff, T. (1989). Polygon scan conversion by exact convolution. In *Proc. of Raster Imaging and Digital Typography*.

- Dukowicz, J. and J. Kodis (1987). Accurate conservative remapping (rezoning) for arbitrary lagrangian-eulerian computations. *SIAM Journal on Scientific and Statistical Computing* 8(3), 305–321.
- Dukowicz, J., N. Padial, and L. A. N. Laboratory (1991). *REMAP3D, a Conservative Three-dimensional Remapping Code*. Los Alamos National Laboratory.
- Eisenberg, M. A. and L. E. Malvern (1973). On finite element integration in natural coordinates. *International Journal for Numerical Methods in Engineering* 7(4), 574–575.
- Garimella, R., M. Kucharik, and M. Shashkov (2007). An efficient linearity and bound preserving conservative interpolation (remapping) on polyhedral meshes. *Computers & Fluids* 36(2), 224 – 237.
- Grandy, J. (1999). Conservative remapping and region overlays by intersecting arbitrary polyhedra. *Journal of Computational Physics* 148(2), 433 – 466.
- Habib, S., V. Morozov, H. Finkel, A. Pope, K. Heitmann, K. Kumaran, T. Peterka, J. Insley, D. Daniel, P. Fasel, N. Frontiere, and Z. Lukic (2012, November). The Universe at Extreme Scale: Multi-Petaflop Sky Simulation on the BG/Q. *ArXiv e-prints*.
- Hahn, O., T. Abel, and R. Kaehler (2013, September). A new approach to simulating collisionless dark matter fluids. *M.N.R.A.S.* 434, 1171–1191.
- Hahn, O. and R. E. Angulo (2015, January). An adaptively refined phase-space element method for cosmological simulations and collisionless dynamics. *ArXiv e-prints*.
- Hahn, O., R. E. Angulo, and T. Abel (2014, April). The Properties of Cosmic Velocity Fields. *ArXiv e-prints*.
- Hasselgren, J., T. Akenine-Möller, and L. Ohlsson (2005). *Conservative Rasterization*, pp. 677–690. GPU Gems 2. Addison-Wesley Professional.
- Hirt, C. and B. Nichols (1981). Volume of fluid (vof) method for the dynamics of free boundaries. *Journal of Computational Physics* 39(1), 201 – 225.
- Hockney, R. W. and J. W. Eastwood (1988). *Computer Simulation Using Particles*. Bristol, PA, USA: Taylor & Francis, Inc.
- Hoffmann, C. M., J. E. Hopcroft, and M. S. Karasick (1988). Towards implementing robust geometric computations. In *Proceedings of the Fourth Annual Symposium on Computational Geometry*, SCG '88, New York, NY, USA, pp. 106–117. ACM.
- Hughes, T. (1981, December). Lagrangian-Eulerian finite element formulation for incompressible viscous flows. *Computer Methods in Applied Mechanics and Engineering* 29, 329–349.
- Jameson, A., W. Schmidt, and E. Turkel (Eds.) (1981, June). *Numerical solution of the Euler equations by finite volume methods using Runge Kutta time stepping schemes*.

- Kaehler, R., O. Hahn, and T. Abel (2012). A novel approach to visualizing dark matter simulations. *IEEE Transactions on Visualization and Computer Graphics* 18(12), 2078–2087.
- Karasick, M. S. (1989). *On the Representation and Manipulation of Rigid Solids*. Ph. D. thesis, Montreal, Que., Canada, Canada. UMI order no: not available.
- Kravtsov, A. V., A. A. Klypin, and A. M. Khokhlov (1997, July). Adaptive Refinement Tree: A New High-Resolution N-Body Code for Cosmological Simulations. *ApJS* 111, 73–94.
- Liggett, J. A. (1988). Exact formulae for areas, volumes and moments of polygons and polyhedra. *Communications in Applied Numerical Methods* 4(6), 815–820.
- Liu, Y. and M. Vinokur (1998). Exact integrations of polynomials and symmetric quadrature formulas over arbitrary polyhedral grids. *Journal of Computational Physics* 140(1), 122–147.
- López, J. and J. Hernández (2008, June). Short note: Analytical and geometrical tools for 3d volume of fluid methods in general grids. *J. Comput. Phys.* 227(12), 5939–5948.
- Loubère, R., P.-H. Maire, M. Shashkov, J. Breil, and S. Galera (2010). Reale: A reconnection-based arbitrary-lagrangian–eulerian method. *Journal of Computational Physics* 229(12), 4724–4761.
- Margolin, L. and M. Shashkov (2003). Second-order sign-preserving conservative interpolation (remapping) on general grids. *Journal of Computational Physics* 184(1), 266 – 298.
- Milenkovic, V. J. (1988). *Verifiable Implementations of Geometric Algorithms Using Finite Precision Arithmetic*. Ph. D. thesis, Pittsburgh, PA, USA. AAI8826536.
- Mirtich, B. (1996, February). Fast and accurate computation of polyhedral mass properties. *J. Graph. Tools* 1(2), 31–50.
- Neyrinck, M. C. (2008, June). ZOBOV: a parameter-free void-finding algorithm. *M.N.R.A.S.* 386, 2101–2109.
- Pantaleoni, J. (2011). Voxelpipe: A programmable pipeline for 3d voxelization. In *Proceedings of the ACM SIGGRAPH Symposium on High Performance Graphics*, HPG '11, New York, NY, USA, pp. 99–106. ACM.
- Renardy, M., Y. Renardy, and J. Li (2001). Numerical simulation of moving contact line problems using a volume-of-fluid method. *Journal of Computational Physics* 171(1), 243 – 263.
- Springel, V. (2005, December). The cosmological simulation code GADGET-2. *M.N.R.A.S.* 364, 1105–1134.
- Springel, V. (2010, January). E pur si muove: Galilean-invariant cosmological hydrodynamical simulations on a moving mesh. *MNRAS* 401, 791–851.

- Steinitz, E. (1922). *Polyeder und Raumeinteilungen*, Volume 3 of *Encyclopädie der mathematischen Wissenschaften*, pp. 1–139. B.G. Teubner Verlag.
- Stephenson, M. B. and H. N. Christiansen (1975, September). A polyhedron clipping and capping algorithm and a display system for three dimensional finite element models. *SIG-GRAPH Comput. Graph.* 9(3), 1–16.
- Stewart, A. J. (1994). Local robustness and its application to polyhedral intersection. *International Journal of Computational Geometry and Applications* 4(1), 87–118.
- Stone, M. G. (1986). A mnemonic for areas of polygons. *Am. Math. Monthly* 93.
- Sugihara, K. (1994). A robust and consistent algorithm for intersecting convex polyhedra. *Computer Graphics Forum* 13(3), 45–54.
- Sugihara, K. and M. Iri (1989). Two design principles of geometric algorithms in finite-precision arithmetic. *Applied Mathematics Letters* 2(2), 203 – 206.
- Sugihara, K. and M. Iri (1990, April). A solid modelling system free from topological inconsistency. *J. Inf. Process.* 12(4), 380–393.
- Sutherland, I. E. and G. W. Hodgman (1974, January). Reentrant polygon clipping. *Commun. ACM* 17(1), 32–42.
- Teyssier, R. (2002, April). Cosmological hydrodynamics with adaptive mesh refinement. A new high resolution code called RAMSES. *A&A* 385, 337–364.
- Warren, M. S. (2013, October). 2HOT: An Improved Parallel Hashed Oct-Tree N-Body Algorithm for Cosmological Simulation. *ArXiv e-prints*.
- Zhang, L., W. Chen, D. S. Ebert, and Q. Peng (2007, August). Conservative voxelization. *Vis. Comput.* 23(9), 783–792.